Materials Research Letters

ISSN: (Print) 2166-3831 (Online) Journal homepage: https://www.tandfonline.com/loi/tmrl20

# Probing the role of Johari–Goldstein relaxation in the plasticity of metallic glasses

M. Zhang, Y. Chen, R. G. He, S. F. Guo, J. Ma & L. H. Dai

**To cite this article:** M. Zhang, Y. Chen, R. G. He, S. F. Guo, J. Ma & L. H. Dai (2019) Probing the role of Johari–Goldstein relaxation in the plasticity of metallic glasses, Materials Research Letters, 7:9, 383-391, DOI: 10.1080/21663831.2019.1620360

**To link to this article:** https://doi.org/10.1080/21663831.2019.1620360



Published online: 22 May 2019.

MATER. RES. LETT.
2019, VOL. 7, NO. 9, 383–391
https://doi.org/10.1080/21663831.2019.1620360

MATERIALS RESEARCH LETTERS
Taylor & Francis
Taylor & Francis Group

ORIGINAL REPORT



# Probing the role of Johari–Goldstein relaxation in the plasticity of metallic glasses

M. Zhang[a,b], Y. Chen[b,c], R. G. He[d], S. F. Guo[d], J. Ma[e] and L. H. Dai[b,c]

[a]Institute of Advanced Wear & Corrosion Resistant and Functional Materials, Jinan University, Guangzhou, People's Republic of China; [b]State Key Laboratory of Nonlinear Mechanics, Institute of Mechanics, Chinese Academy of Sciences, Beijing, People's Republic of China; [c]School of Engineering Sciences, University of Chinese Academy of Sciences, Beijing, People's Republic of China; [d]Faculty of Materials and Energy, Southwest University, Chongqing, People's Republic of China; [e]Guangdong Provincial Key Laboratory of Micro/Nano Optomechatronics Engineering, College of Mechatronics and Control Engineering, Shenzhen University, Shenzhen, People's Republic of China

**ABSTRACT**

Johari–Goldstein (JG) relaxation closely relates to the shear transformation zones (STZs) in the flow of metallic glasses (MGs). However, the actual role played by JG relaxation in the STZ-evoked plastic deformation of MGs remains unknown. In this work, by substituting the transition metal (TM) element in La(TM)Al MGs (TM = Ni, Co, Cu, CuNi) to tune the feature of JG relaxation, how JG relaxation alters the deformation behaviors of MGs is tentatively examined with nanoindentation. The results demonstrate that JG relaxation modulates the anelastic to plastic transition rate in the plastic deformation accommodation of MGs via a characteristic relaxation time.

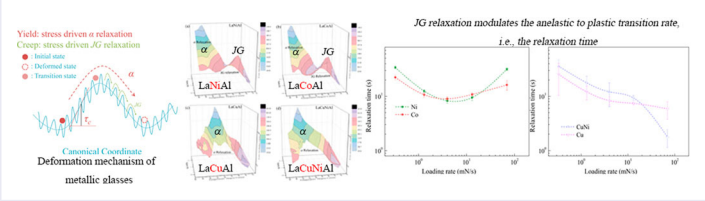


**IMPACT STATEMENT**

A characteristic relaxation time revealing the role of Johari–Goldstein relaxation in the plasticity of metallic glasses as modulating the anelastic to plastic transition rate is characterized.

**ARTICLE HISTORY**
Received 21 December 2018

**KEYWORDS**
Metallic glasses; Johari–Goldstein relaxation; plasticity; nanoindentation

## 1. Introduction

Due to the lack of well-defined structural defects (like dislocations and twins) to accommodate plastic deformation [1,2], how to exploit the ductility of metallic glasses (MGs) stands as an unsolved mystery [3,4]. In order to establish the plastic deformation accommodation mechanisms in MGs, conceived phenomenological defect has been proposed as shear transformation zones (STZ) [5] or flow units [6], however, both stay conceptual and are yet to be identified [7,8]. To relate STZ to the physical properties of MGs, Harmon et al. [9] proposed a potential–energy–landscape (PEL) perspective on the plastic deformation accommodation mechanisms of MGs. As illustrated in Figure 1, on the PEL, the plastic deformation in MGs can be viewed as a stress-driven $\alpha$ relaxation process (as indicated by the red dashed arrow) during which global irreversible atomic rearrangements are activated. As identified by Debenedetti and Stillinger [10], on the PEL, the primary $\alpha$ relaxation is composed of a group of consecutive Johari–Goldstein (JG) relaxations (as indicated by the green dashed arrows) where local reversible atomic rearrangements underly. Thereby, Harmon et al. successfully associated STZ, the conceived plastic deformation accommodation defect, with JG relaxation via examining the iso-configurational shear modulus and recovery enthalpy in the anelastic to plastic transition in

**CONTACT** M. Zhang m.zhangiwrm@jnu.edu.cn Institute of Advanced Wear & Corrosion Resistant and Functional Materials, Jinan University, Guangzhou 510632, People's Republic of China; State Key Laboratory of Nonlinear Mechanics, Institute of Mechanics, Chinese Academy of Sciences, Beijing 100190, People's Republic of China; Y. Chen chenyan@lnm.imech.ac.cn State Key Laboratory of Nonlinear Mechanics, Institute of Mechanics, Chinese Academy of Sciences, Beijing 100190, People's Republic of China; School of Engineering Sciences, University of Chinese Academy of Sciences, Beijing 100049, People's Republic of China; L. H. Dai lhdai@lnm.imech.ac.cn State Key Laboratory of Nonlinear Mechanics, Institute of Mechanics, Chinese Academy of Sciences, Beijing 100190, People's Republic of China; School of Engineering Sciences, University of Chinese Academy of Sciences, Beijing 100049, People's Republic of China

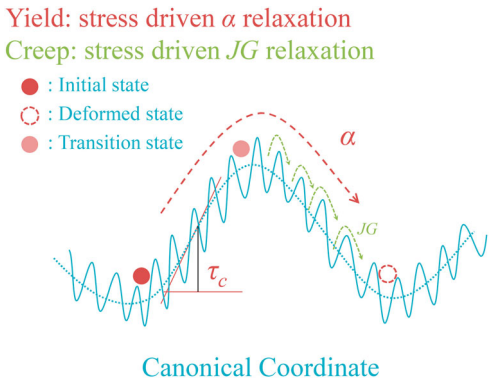


**Figure 1.** Plastic deformation accommodation mechanisms in the flow of metallic glasses (MGs). On the potential energy landscape, the flow of MGs can be understood as a stress-driven $\alpha$ relaxation process (as indicated by the red dashed arrow). The $\alpha$ relaxation is conceived as composed of Johari–Goldstein (JG) relaxations (as indicated by the green dashed arrows). In the creep stage of nanoindentation, the MG beneath the indenter is post-yield and close to the transition state ($\tau_c$ is the yield stress). Thus, the deformation in the creep stage of nanoindentation reveals the plastic deformation accommodation character of MGs and can be considered as stress driven JG relaxations.

MGs [9]. The STZ-mediated plastic deformation accommodation of MGs is suggested to be an anelastic to plastic transition via consecutive JG relaxations. This is where JG relaxation comes into the plasticity of MGs. Up until now, although expanding evidences indicate that the ductility of MGs might reside in pronounced JG relaxation of MGs [11–13], still under debate is the actual role played in plastic deformation by the mysterious JG relaxation [14–19].

In this work, we aim to probe the actual role of JG relaxation in the plastic deformation of MGs by virtue of the PEL perspective proposed by Harmon et al. [9]. As shown in Figure 1, the plastic deformation of MGs can be described in more details. The maximum of the slop of the PEL defines the yield stress of MGs. Under external loads above the yield stress, the MG system will deviate from the initial energy minimum state and approximate the transition state. With proper assistance from thermal energy fluctuation, the system would hop across the energy barrier and explore nearby energy minimums, i.e. stress-driven $\alpha$ relaxation. Thus, two deformation stages consisting of consecutive JG relaxations can be identified: an anelastic stage (i.e. from the initial state to the transition state) where reversibility is maintained and a plastic stage (i.e. from the transition state to the deformed state) where irreversibility emerges. Since irreversibility is intrinsic to plasticity, to probe the role of JG relaxation in the plasticity of MGs, a prompt idea is to examine the role of JG relaxation in the second deformation stage, where the anelastic to the plastic transition of MGs occurs.

As shown in Figure 1, if the deformed state were considered as the initial undeformed state, the second deformation stage is virtually an inverse of the first deformation stage. Thus, the second deformation stage actually involves the anelastic deformation of MGs which is being plastically deformed. This is exactly the scenario in the creep stage of nanoindentation [20,21], which characterizes the anelastic deformation behaviors of materials being plastically deformed underneath the indenter. Therefore, the deformation behavior in the creep stage of nanoindentation should reveal the strain accommodation character of MGs and would be directly affected by JG relaxation. Hence, to probe the role of JG relaxation in the plasticity of MGs, the La MGs with distinct JG relaxation features [22] as well as excellent glass forming abilities [23] are selected for nanoindentation tests. In order to tune the feature of JG relaxation, different transition metal elements (Ni, Co, Cu, NiCu) are selected to alloy with the La-based MGs [23].

## 2. Materials and methods

Alloy sheets of $1 \times 10 \times 50\,mm^3$ in size with nominal composition $La_{66}Ni_{19}Al_{15}$, $La_{69}Co_{17}Al_{14}$, $La_{66}Cu_{20}Al_{14}$, $La_{57.5}Cu_{12.5}Ni_{12.5}Al_{17.5}$ (at.%) are prepared by copper mold casting. The amorphous structure of the prepared alloys are examined by X-ray Diffraction (Cu-K$\alpha$ Rigaku smartlab IV) and Differential Scanning Calorimeter (Mettler Toledo STA3.0). Nanoindentation tests are conducted on an Agilent G200 Nanoindenter with a Berkovich diamond tip. Load control mode and a group of loading rates $\dot{\boldsymbol{P}}$: 0.33, 1.32, 4, 13.2, and 70 mN/s are selected. The nanoindentation test is composed by loading to a maximum load $P_{max}$ of 200 mN at a constant loading rate; maintaining the load for 10 s at $P_{max}$; unloading to 10% of $P_{max}$ at a rate of 10mN/s; holding the load for 10 s to perform thermal drift calibration, and unloading completely. To guarantee the reliability of the results, each test is repeated seven times. A typical dwell period of 10 s for the creep stage is selected for the materials underneath the indenter to reach a steady mechanical state [24].

## 3. Results and discussion

Figure 2 shows the spectroscopy of loss modulus in the temperature and frequency domain for the 4 La-based MGs. It can be seen that the loss modulus spectroscopies of the 4 La-based MGs manifest distinct characteristics. In Figure 2(a,b), two main peaks can be clearly identified

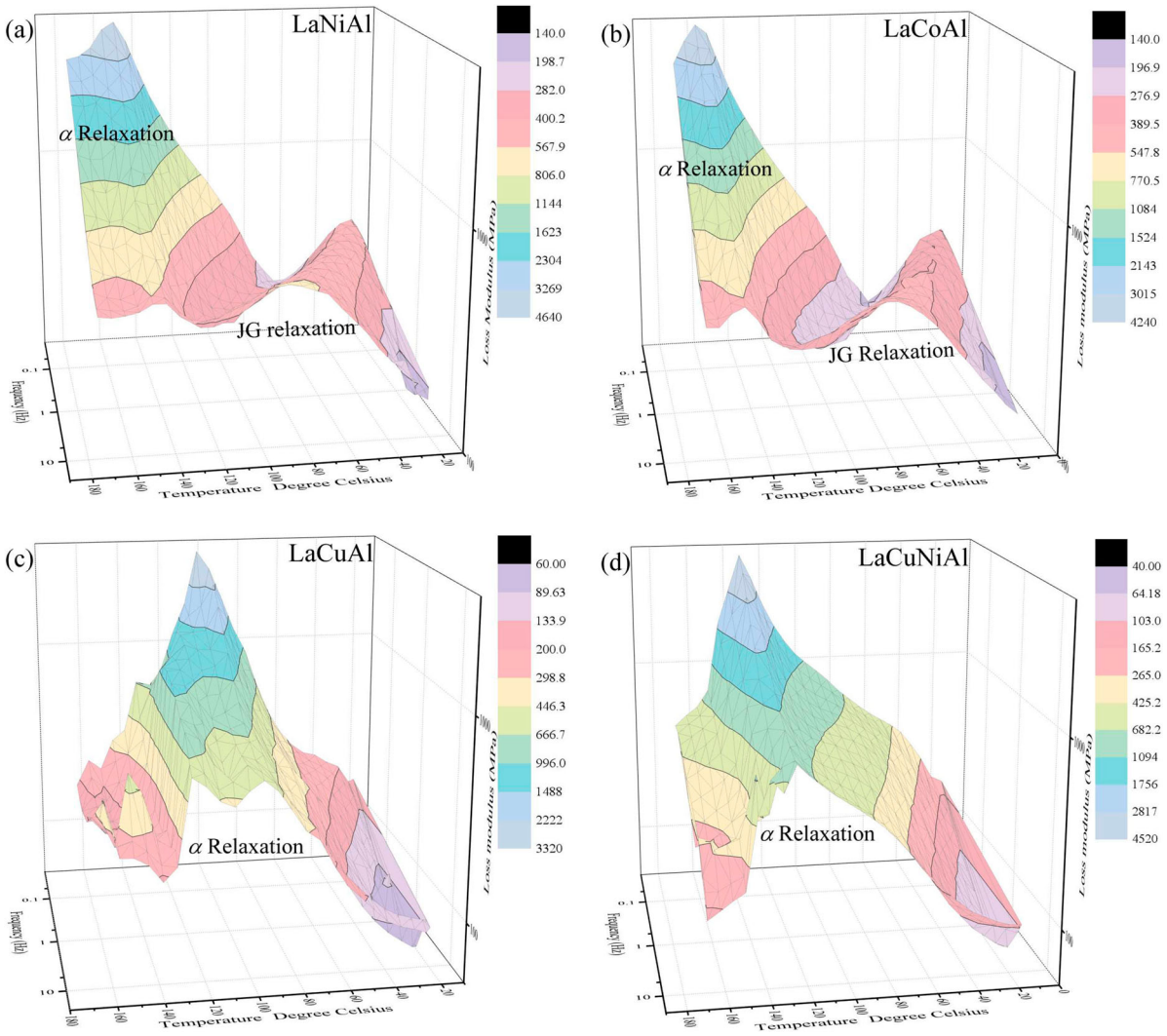


**Figure 2.** The Johari–Goldstein (JG) relaxation of 4 La(TM)Al metallic glasses(MGs), TM = Ni, Co, Cu, CuNi: the loss modulus spectroscopies of the LaNiAl (a) and LaCoAl (b) MGs with pronounced JG relaxation, and of the LaCuAl (c) and LaCuNiAl (d) MGs without pronounced JG relaxation.

for the LaNiAl and LaCoAl MGs. A peak in the high-temperature region corresponds to the thermal glass transition, i.e. the primary $\alpha$ relaxation. On the other hand, a pronounced secondary peak at relatively lower temperature corresponds to the JG relaxation. However, in Figure 2(c,d), only the $\alpha$ relaxation peak could be resolved for the LaCuAl and LaCuNiAl MGs. As for the JG relaxation, merely an excess wing clinging to the $\alpha$ relaxation peak can be found. These results confirm that the prepared MGs display different JG relaxation features, as having been reported previously [22].

Figure 3(a–d) shows the typical load ($P$) vs. displacement ($h$) curves of the 4 La-based MGs in nanoindentation under different loading rates. For clarity, the curves are shifted along the transversal axis according to the loading rate, i.e. from left to right: 70 mN/s to 0.33 mN/s. It can be seen in Figure 3(a,b) that, with increasing loading rate, moderate serrations emerge and increase on the $P$-$h$ curves for the LaNiAl ($T_g$ = 426 K) and LaCoAl ($T_g$ = 433 K) MGs [25], where $T_g$ is the glass transition temperature. On the other hand, in Figure 3(c,d), prominent serrations can be found on the $P$–$h$ curves of the LaCuAl ($T_g$ = 370 K) and LaCuNiAl ($T_g$ = 430 K) MGs, but decrease with increasing loading rate. For a better view on the serrations, the $P$-$h$ curves are subtracted by their power law fit [21], as shown in Figure 3(e–h). Noting $T_g$ of the LaCuAl and LaCuNiAl MGs, the moderate serrations for LaNiAl and LaCoAl MGs are clearly not because of their low $T_g$. According to the stick-slip model [26], the increasing serrations on the curves are attributed to the retarded deformation accommodation process relative to the loading rate, i.e. the retarded anelastic to plastic transition, and *vice versa*. This explanation has been proved in model glasses [27], where the serrations arise

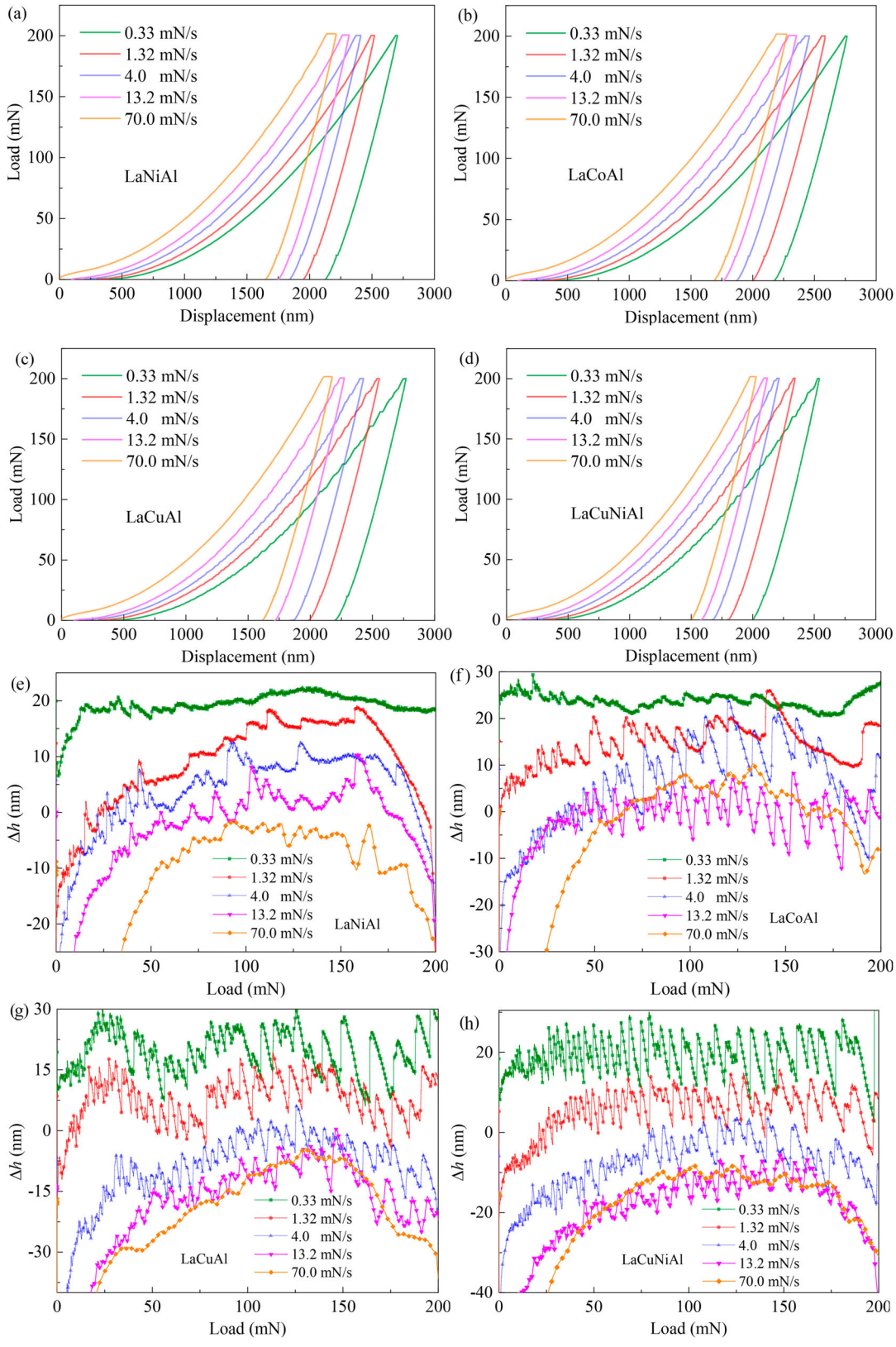


**Figure 3.** The load–displacement curves of the 4 La(TM)Al metallic glasses (MGs), TM = Ni, Co, Cu, CuNi: (a) LaNiAl, (b) LaCoAl, (c) LaCuAl, and (d) LaCuNiAl. The serrations of the four La (TM)Al MGs: (e) LaNiAl, (f) LaCoAl, (g) LaCuAl, and (h) LaCuNiAl. Upon increased loading rate, increasing serrations can be found for the LaNiAl and LaCoAl MGs, while decreasing serrations can be observed for the LaCuAl and LaCuNiAl MGs.

from the local avalanche of the atoms to abruptly accommodate plastic deformation. As illustrated in Figure 1, the plastic deformation accommodation process in MGs consists of consecutive JG relaxations. Therefore, the different serrations on the *P-h* curves of the 4 MGs should probably originate from their different JG relaxation characteristics. It is intriguing to note that, for all 4 La MGs, at the loading rate 70 mN/s, the serrations exhibit an abrupt decrease. This is plausibly due to the superimposition of serrations under high loading rates [28], where the following serration emerges before the preceding serration fully develops, as suggested by the increased width of the serrations. More works on the decrease of serrations of MGs under high loading rates to illustrate this phenomenon are worth conducting in future.

Figure 4(a–d) shows the creep displacement *vs*. time curves of the 4 La-based MGs in the creep stage of nanoindentation extracted from Figure 3. The solid points are experimental results and the solid lines are the numerical fits. It can be found that, with increasing loading rate, the creep displacement increases for all the 4 MGs. To reveal the underlying deformation dynamics, the creep displacement *vs*. time curves are fitted with the Kohlrausch–Williams–Watts (KWW) equation [29]: $h_c = h_0(1 - \exp(-(t/\tau_r)^{\beta}))$, where $h_c$ is the time-dependent creep displacement; $h_0$ is the total creep displacement, $\tau_r$ is the relaxation time which measures the rate of the creep deformation, and $\beta$ is the stretched exponent representing the deviation of the creep behavior from the exponential process. It can be seen that all the experimental results exhibits good agreements with the KWW fits, suggesting the applicability of KWW equation to characterizing the deformation behaviors of the 4 La-based MGs [21].

Figure 4(e,f) shows the stretched exponent $\beta$ and the relaxation time $\tau_r$ of the 4 La-based MGs. The lines are eye guides. It can be seen in Figure 4(e) that the stretched exponents for the 4 MGs decrease similarly from $\sim$1.2 to $\sim$0.2 at increasing loading rate. This result is consistent with previous observations made with different methods [30]. Upon increasing loading rate, the decreasing of $\beta$ indicates a stretched-exponentially increasing behavior of the creep displacement and suggests that the activation energies of the STZ of the 4 MGs follow a broader distribution at higher loading rates [31]. The concordant decreasing of $\beta$ in Figure 4(e) suggests that the four MGs exhibit similar heterogeneity in the thermally activated STZs nucleation dynamics. Intriguingly, as shown in Figure 4(f), the relaxation times for the 4 La MGs show slightly different evolution phenomena with increasing loading rate. For clarity, the relaxation times are shown separately in Figure 4(g) for the LaNiAl and LaCoAl MGs, and Figure 4(h) for the LaCuAl and LaCuNiAl MGs. Two different tendencies can be observed: for the Ni and Co alloyed La MGs, the relaxation time remains above $\sim$10 s, indicating an almost unchanged deformation accommodation rate, i.e. increasing serrations under increasing loading rate; however, for the Cu and CuNi alloyed La MGs, the relaxation times decrease similarly and monotonously from $\sim$30 to $\sim$3 s, manifesting an increased deformation accommodation rate, i.e. decreasing serrations under increasing loading rate. The observations in Figure 4 are consistent with the serrations observed in Figure 3.

As proposed previously, the deformation of MGs in the creep stage of nanoindentation actually stems from the plastic deformation accommodation process where the system explores the neighborhood energy minimum via consecutive JG relaxations. The relaxation time $\tau_r$ for the MGs is thus closely related to the JG-relaxation and characterize the *local and microscopic* anelastic to plastic transition rate. By probing $\tau_r$ of the 4 La MGs, it is concluded that the role of JG relaxation in the plasticity of MGs involves modulating the plastic deformation accommodation rate via the operations of STZs. This is probably why consistent activation energy values were identified for these two fundamentally correlated processes, i.e. STZ and JG relaxation [12]. Why pronounced JG relaxation would lead to a nearly constant relaxation time is worth intensive investigations resorting to molecular simulations in the future. The relaxation time would be a helpful physical property to understanding the perplexing nature of JG relaxation in amorphous materials [15–17].

To evaluate the effect of JG relaxation on the macroscopic plasticity of MGs, Figure 5 shows the typical load-displacement curves of the 4 La MGs in quasi-static compression and the corresponding fracture surface morphologies. In Figure 5(a), it can be seen that all the 4 La MGs exhibit macroscopic brittle fracture and nearly none plastic deformation. Based on the typical 'dimple' features on the fracture surface in Figure 5(b), all the 4 La MG exhibits similar microscopic ductile fracture behavior. It is noted that, in the enlarged images of the fracture surface on the right side, the higher ratio of the area of 'smooth' regions vs. the area of 'dimpled' regions on the fracture surface of the LaNiAl and LaCoAl MGs is due to the limited area of the region on the fracture surface selected to take the image. As a whole, rather similar ratios of the area of 'smooth' regions vs. the area of 'dimpled' regions of the four La MGs can be observed on the entire fracture surface shown in the low magnification images on the left side. Nevertheless, since the 'smooth' region and the 'dimpled' region should probably relate to the tension transformation zone (TTZ) [32] and the STZ respectively, detailed correlations between JG relaxation

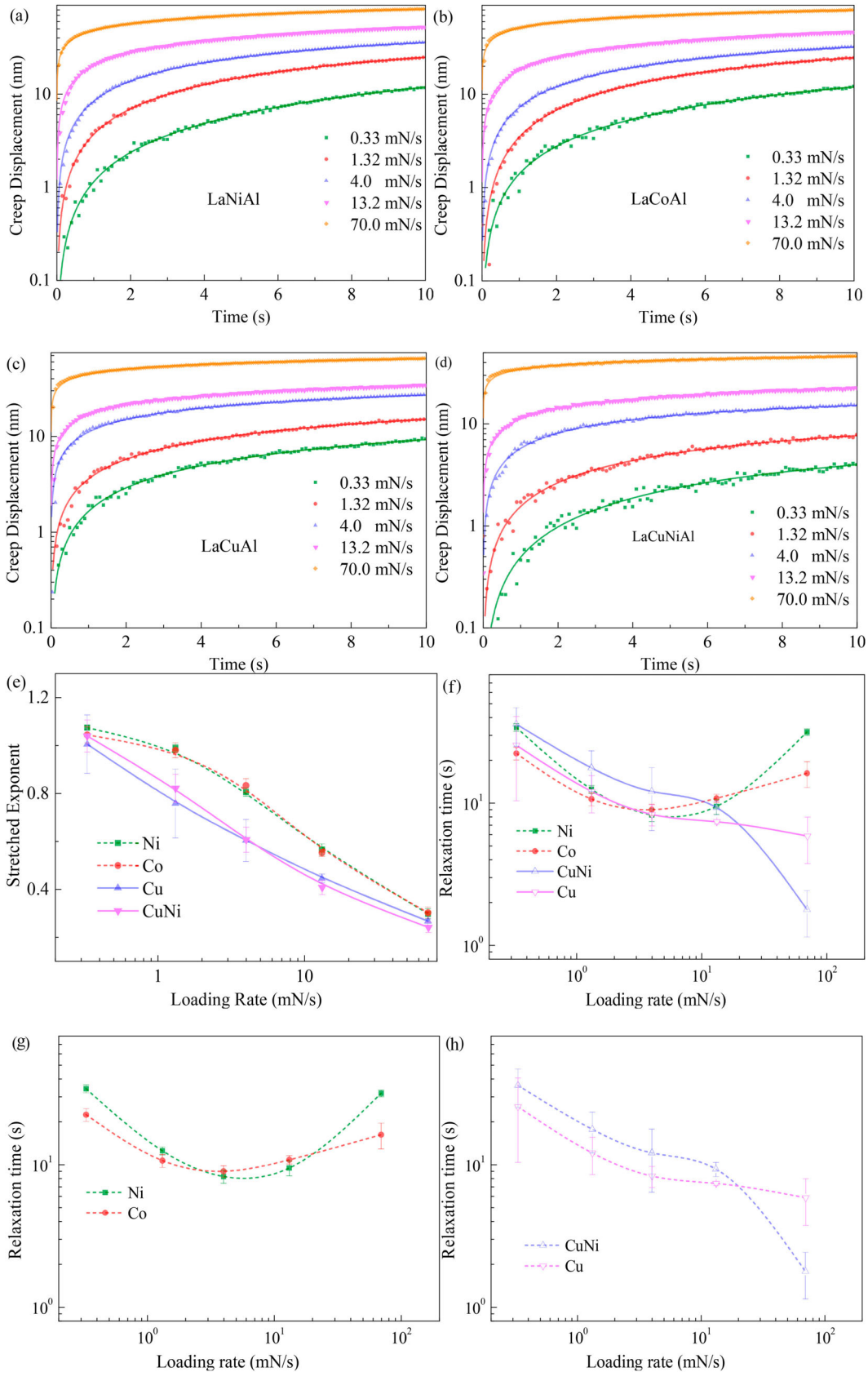


**Figure 4.** Creep displacement *vs*. time curves of the 4 La(TM)Al metallic glasses (MGs), TM = Ni, Co, Cu, CuNi, in the creep stage of nanoindentation with the maximum load reached at different loading rates: (a) LaNiAl, (b) LaCoAl, (c) LaCuAl, and (d) LaCuNiAl. Solid lines are the Kohlrausch–Williams–Watts (KWW) equation fits. Stretched exponent $\beta$ (e) and relaxation time (f) of the La(TM)Al MGs derived from the KWW equation fits. The relaxation time of Ni and Co alloyed MGs (g) nearly remains a constant, while the relaxation time of the Cu and CuNi alloyed MGs (h) display a clear decrease, under increasing loading rate.

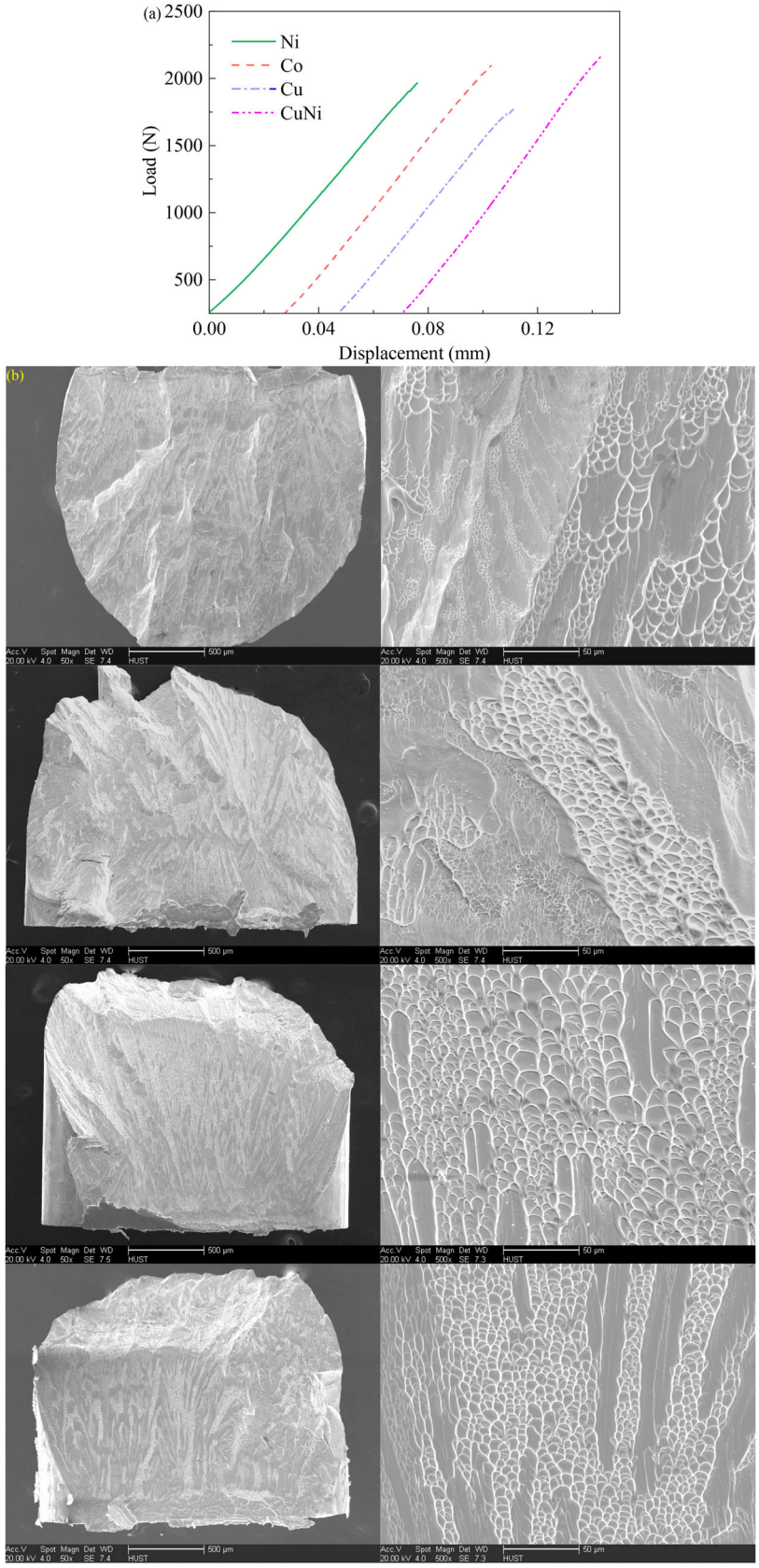


**Figure 5.** Typical compression curves of the 4 La(TM)Al metallic glasses (MGs), TM = Ni, Co, Cu, CuNi, (a) and the typical fractography (b), from top to bottom: TM = Ni, Co, Cu, CuNi.

and the fracture of MGs are to be explored in our future works. These results suggest that the pronounced JG-relaxation might affect the deformation accommodation mechanisms of MGs as well, yet is not the unique factor that determines the macroscopic plasticity of MGs [11]. For example, the effect of loading rate is probably critical [1]. Therefore, more issues involved in the ductility of MGs are to be determined in the future.

## 4. Conclusions

In summary, the deformation behaviors of La(TM)Al (TM = Ni, Cu, Co, NiCu) MGs with different JG relaxation characteristics are characterized by nanoindentation. With pronounced JG relaxation, the La MGs exhibit increasing serrations with increasing loading rate in the loading stage, and exhibit an almost constant relaxation time in the creep stage regardless of the loading rate at which the maximum load is reached. While without pronounced JG relaxation, the La MGs exhibit decreasing serrations with increasing loading rate in the loading stage and exhibit a decreasing relaxation time in the creep stage when the maximum load is reached at increasing loading rate. These results indicate that JG relaxation modulates the deformation accommodation rate in the plasticity of MGs and underpins the fundamental relationship between JG relaxation and STZ.

## Disclosure statement

No potential conflict of interest was reported by the authors.

## Funding

This work was financially supported by the National Nature and Science Foundation of China [grant number 51701082], 'the Fundamental Research Funds for the Central Universities' and the Guangdong Province Science and Technology Plan [grant number 2017B090903005]. M. Z. and Y. C. are also grateful for the support of the Opening Fund of State Key Laboratory of Non-linear Mechanics [grant number LNM201812].

## References

[1] Spaepen F. A microscopic mechanism for steady state inhomogeneous flow in metallic glasses. Acta Metall. 1977;25:407–415.
[2] Argon AS. Plastic deformation in metallic glasses. Acta Metall. 1979;27:47–58.
[3] Ketov SV, Sun YH, Nachum S, et al. Rejuvenation of metallic glasses by non-affine thermal strain. Nature. 2015;524:200.
[4] Wang ZT, Pan J, Li Y, et al. Densification and strain hardening of a metallic glass under tension at room temperature. Phys Rev Lett. 2013;111:135504.
[5] Langer JS. Dynamics of shear-transformation zones in amorphous plasticity: Formulation in terms of an effective disorder temperature. Phys Rev E. 2004;70:041502.
[6] Wang Z, Wen P, Huo LS, et al. Signature of viscous flow units in apparent elastic regime of metallic glasses. Appl Phys Lett. 2012;101.
[7] Xu B, Falk ML, Li JF, et al. Predicting shear transformation events in metallic glasses. Phys Rev Lett. 2018;120:5.
[8] Peng HL, Li MZ, Wang WH. Structural signature of plastic deformation in metallic glasses. Phys Rev Lett. 2011;106:135503.
[9] Harmon JS, Demetriou MD, Johnson WL, et al. Anelastic to plastic transition in metallic glass-forming liquids. Phys Rev Lett. 2007;99:135502.
[10] Debenedetti PG, Stillinger FH. Supercooled liquids and the glass transition. Nature. 2001;410:259–267.
[11] Yu HB, Shen X, Wang Z, et al. Tensile plasticity in metallic glasses with pronounced $\beta$ relaxations. Phys Rev Lett. 2012;108:015504.
[12] Yu HB, Wang WH, Bai HY, et al. Relating activation of shear transformation zones to beta relaxations in metallic glasses. Phys Rev B. 2010;81:220201.
[13] Wang Q, Liu JJ, Ye YF, et al. Universal secondary relaxation and unusual brittle-to-ductile transition in metallic glasses. Mater Today. 2017;20:293–300.
[14] Cui BY, Evenson Z, Fan BB, et al. Possible origin of beta-relaxation in amorphous metal alloys from atomic-mass differences of the constituents. Phys Rev B. 2018;98:7.
[15] Bi QL, Lu YJ, Wang WH. Multiscale relaxation dynamics in ultrathin metallic glass-forming films. Phys Rev Lett. 2018;120:6.
[16] Wang XD, Zhang J, Xu TD, et al. Structural signature of beta-relaxation in La-based metallic glasses. J Phys Chem Lett. 2018;9:4308–4313.
[17] Yu HB, Yang MH, Sun Y, et al. Fundamental link between beta relaxation, excess wings, and cage-breaking in metallic glasses. J Phys Chem Lett. 2018;9:5877–5883.
[18] Zhu F, Nguyen HK, Song SX, et al. Intrinsic correlation between beta-relaxation and spatial heterogeneity in a metallic glass. Nat Commun. 2016;7:11516.
[19] Lu Z, Shang BS, Sun YT, et al. Revealing beta-relaxation mechanism based on energy distribution of flow units in metallic glass. J. Chem. Phys. 2016;144.
[20] Zhang M, Chen Y, Wei D, et al. Extraordinary creep relaxation time in a La-based metallic glass. J Mater Sci. 2018;53:2956–2964.
[21] Zhang M, Wang YJ, Dai LH. Understanding the serrated flow and Johari-Goldstein relaxation of metallic glasses. J Non-Cryst Solids. 2016;444:23–30.
[22] Wang Z, Yu HB, Wen P, et al. Pronounced slow $\beta$-relaxation in La-based bulk metallic glasses. J Phys: Condens Matter. 2011;23:142202.
[23] Yang H, Li X, Li Y. The effect of various transition metals on glass formation in ternary La-TM-Al (TM = Co, Ni, Cu) alloys. J Mater Res. 2011;26:992–996.
[24] Wei BC, Zhang LC, Zhang TH, et al. Strain rate dependence of plastic flow in Ce-based bulk metallic glass during nanoindentation. J Mater Res. 2007;22:258–263.
[25] Schuh CA, Nieh TG, Kawamura Y. Rate dependence of serrated flow during nanoindentation of a bulk metallic glass. J Mater Res. 2002;17:1651–1654.
[26] Klaumünzer D, Maaß R, Löffler JF. Stick-slip dynamics and recent insights into shear banding in metallic glasses. J. Mater. Res. 2011;26:1453–1463.

[27] Murali P, Ramamurty U, Shenoy VB. Strain accommodation in inelastic deformation of glasses. Phys Rev B. 2007;75:024203.
[28] Lemaitre A, Caroli C. Rate-dependent avalanche size in athermally sheared amorphous solids. Phys Rev Lett. 2009;103:4.
[29] Williams G, Watts DC. Non-symmetrical dielectric relaxation behaviour arising from a simple empirical decay function. Trans Faraday Soc. 1970;66:80–85.
[30] Luttich M, Giordano VM, Le Floch S, et al. Anti-aging in ultrastable metallic glasses. Phys Rev Lett. 2018;120:135504.
[31] Wang Z, Sun BA, Bai HY, et al. Evolution of hidden localized flow during glass-to-liquid transition in metallic glass. Nat Commun. 2014;5:5823.
[32] Jiang MQ, Ling Z, Meng JX, et al. Energy dissipation in fracture of bulk metallic glasses via inherent competition between local softening and quasi-cleavage. Philos Mag. 2008;88:407–426.